# *Supporting Information for*:

## Actinide complexes with Wells-Dawson Polyoxometalates (Part 1): Americium and Curium

Ian Colliard* and Gauthier J.-P. Deblonde*

Lawrence Livermore National Laboratory, Livermore, California 94550, USA

*Colliard1@LLNL.gov ; Deblonde1@LLNL.gov

**Table S1.** Select bond distances and structural parameters for the lanthanide(III) complexes of $P_2W_{17}$ previously reported in the literature.

| | **La($P_2W_{17}$)$_2$** | **Pr($P_2W_{17}$)$_2$** | **Nd($P_2W_{17}$)$_2$** | **Eu($P_2W_{17}$)$_2$** | **Gd($P_2W_{17}$)$_2$** | **Tb($P_2W_{17}$)$_2$** | **Dy($P_2W_{17}$)$_2$** | **Yb($P_2W_{17}$)$_2$** | **Lu($P_2W_{17}$)$_2$** |
|---|---|---|---|---|---|---|---|---|---|
| Formula | $K_5Na_6(H_3O)_6[La(P_2W_{17}O_{61})_2]\cdot 49H_2O$ | $K_{17}[Pr(P_2W_{17}O_{61})_2]\cdot nH_2O$ | $K_{17}[Nd(P_2W_{17}O_{61})_2]\cdot 4H_2O$ | $K_{16}H[Eu(P_2W_{17}O_{61})_2]\cdot 43.5H_2O$ | $K_{17}[Gd(P_2W_{17}O_{61})_2]\cdot 26H_2O$ | $K_{17}[Tb(P_2W_{17}O_{61})_2]\cdot 53H_2O$ | $K_{17}[Dy(P_2W_{17}O_{61})_2]\cdot 52H_2O$ | $K_{16}H[Yb(P_2W_{17}O_{61})_2]\cdot 44H_2O$ | $K_{17}[Lu(P_2W_{17}O_{61})_2]\cdot 54H_2O$ |
| Crystal system | triclinic | Monoclinic | triclinic | triclinic | triclinic | triclinic | triclinic | triclinic | triclinic |
| Space group | *P*–1 | *P* 21/*n* | *P*–1 | *P*–1 | *P*–1 | *P*–1 | *P*–1 | *P*–1 | *P*–1 |
| Average bond <M-O> | 2.480 | 2.471 Å | 2.445 Å | 2.388 Å | 2.382 Å | 2.384 Å | 2.363 Å | 2.337 Å | 2.318 Å |
| Bent angle P1-Am-P1’ | a | 169.3˚ | 160.0˚ | a | a | 160.2˚ | 160.1˚ | 160.3˚ | 159.7˚ |
| Bent angle P2-Am-P2’ | a | 138.6˚ | 128.5˚ | a | a | 128.5˚ | 128.6˚ | 128.6˚ | 128.2˚ |
| Reference. | Zhang et al.[1] 2006 | This work | This work | Zhang et al.[1] 2006 | Zhang et al.[1] 2006 | Hirakawa et al.[2] 2025 | Hirakawa et al.[2] 2025 | Niu et al.[3] 2004 | Luo et al.[4] 2001 |

a: no CIF file available but the bond distances and crystal structure refinement available in the article from Zhang et al.[1]

**Table S2.** Trivalent and tetravalent actinide complexes with the Wells-Dawson POM that have been isolated and characterized.

| Type | Cation | Compound formula | Ref. |
|---|---|---|---|
| Actinide(III) | $Am^{3+}$ | $K_{17}Am(P_2W_{17}O_{61})_2 \cdot 42.5H_2O$ | This work |
| | | $K_{17}Am(P_2W_{17}O_{61})_2 \cdot 12H_2O$ | |
| | $Cm^{3+}$ | $K_{17}Cm(P_2W_{17}O_{61})_2 \cdot 8H_2O$ | |
| Actinide(IV) | $Th^{4+}$ | $H_{10}K_6Th(P_2W_{17}O_{61})_2 \cdot 26H_2O$ | 5 |
| | $U^{4+}$ | $H_4K_{12}U(P_2W_{17}O_{61})_2 \cdot 32H_2O$ | 5 |
| | | $K_{16}U(P_2W_{17}O_{61})_2 \cdot 22H_2O$ | 6 |
| | $Np^{4+}$ | $K_{16}Np(P_2W_{17}O_{61})_2 \cdot 42H_2O$ | 5 |
| | $Pu^{4+}$ | $H_4K_{12}Pu(P_2W_{17}O_{61})_2 \cdot 19H_2O$ | 5 |
| | $Am^{4+}$ | $H_6K_{10}Am(P_2W_{17}O_{61})_2 \cdot 30H_2O$ | 5 |

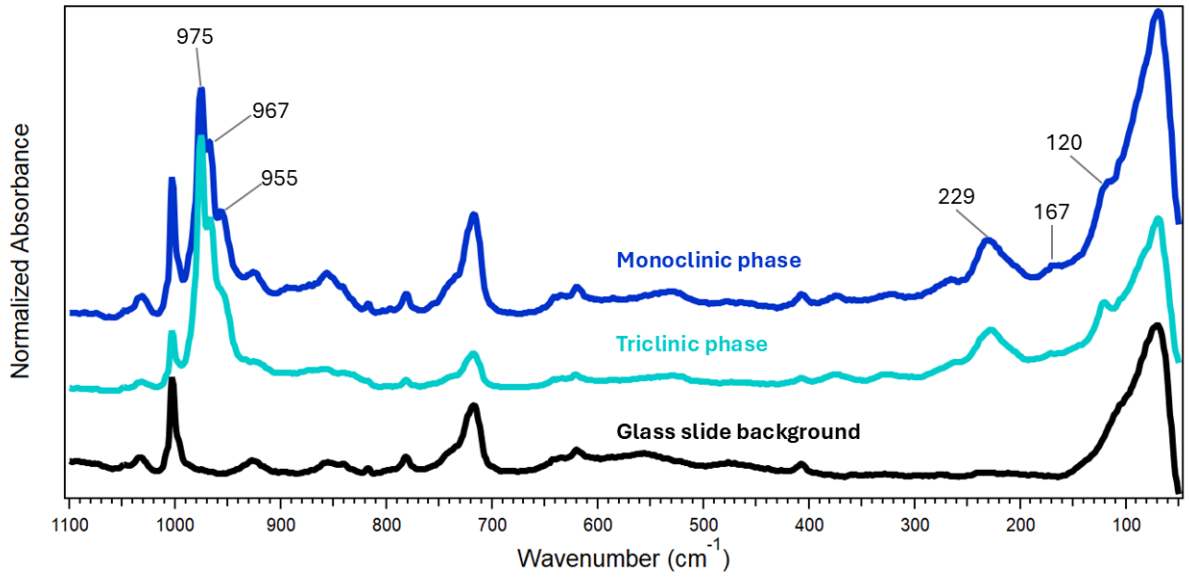


**Figure S1.** Solid-state Raman Spectra for each phase of $Am(P_2W_{17})_2$.

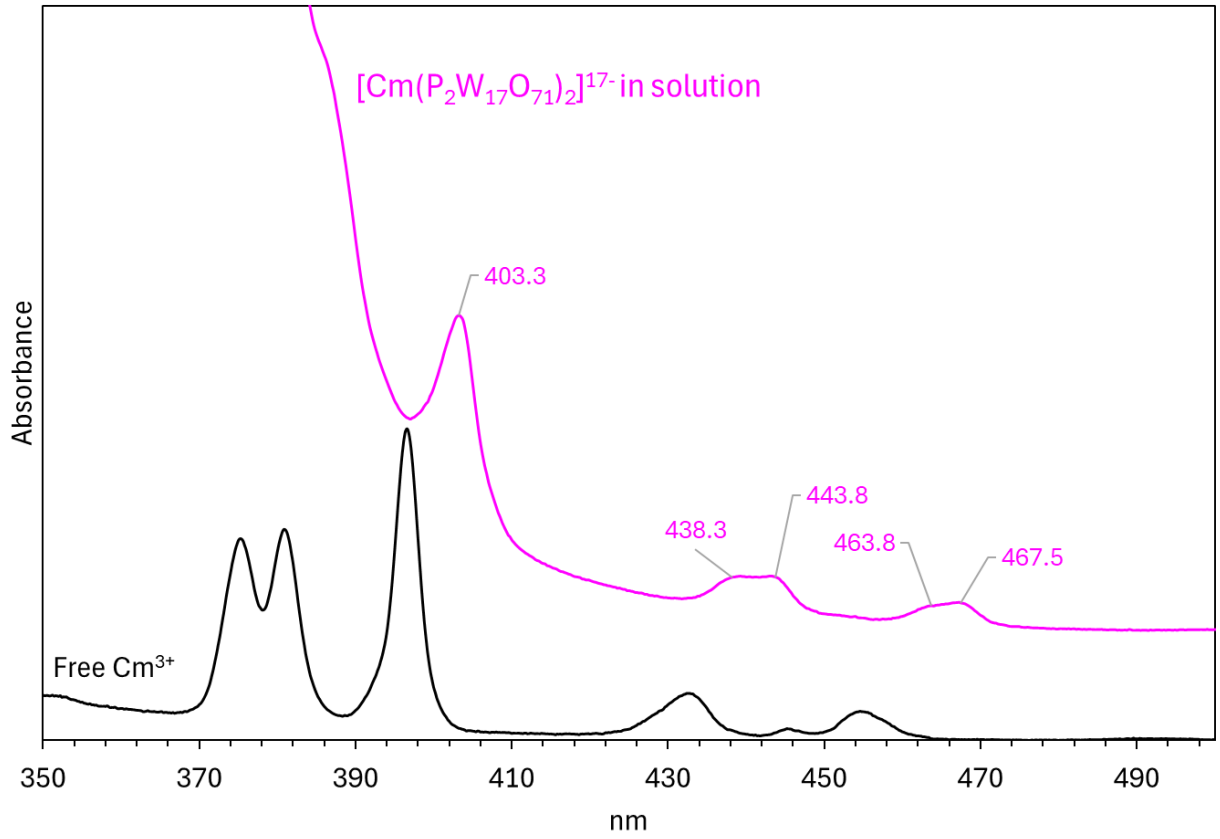


**Figure S2.** Solution-state UV-vis-NIR absorbance spectrum of $[Cm(P_2W_{17})_2]^{17-}$, and uncomplexed $Cm^{3+}$, for comparison.

**Table S3.** Crystallographic table of the Am(III) and Cm(III) complexes of $P_2W_{17}$.

| Identification code | AmP2W17_K_aP | AmP2W17_K_mP | CmP2W17_K_mono |
|---|---|---|---|
| Empirical formula | $Am_2K_{34}O_{305}P_8W_{68}$ | $AmK_{17}O_{122}P_4W_{34}$ | $CmK_{16}O_{122}P_4W_{34}$ |
| Formula weight | 19444.96 | 9234.48 | 9196.38 |
| CCDC ID | 2513146 | 2513147 | 2513143 |
| Temperature/K | 298 | 298 | 298 |
| Crystal system | triclinic | monoclinic | monoclinic |
| Space group | P-1 | $P2_1/n$ | $P2_1/n$ |
| a/Å | 14.6766(2) | 12.3466(3) | 12.36979(18) |
| b/Å | 22.5897(3) | 23.4925(5) | 23.4762(4) |
| c/Å | 24.8555(3) | 51.9402(12) | 51.8839(8) |
| α/° | 95.4060(10) | 90 | 90 |
| β/° | 102.7990(10) | 89.449(2) | 89.4045(14) |
| γ/° | 99.5440(10) | 90 | 90 |
| Volume/Å$^3$ | 7850.80(18) | 15064.7(6) | 15066.1(4) |
| Z | 1 | 4 | 4 |
| $\rho_{calc}$g/cm$^3$ | 4.113 | 4.072 | 4.054 |
| μ/mm$^{-1}$ | 25.876 | 26.944 | 26.945 |
| F(000) | 8428 | 15880 | 15808.0 |
| Crystal size/mm$^3$ | 0.407 × 0.248 × 0.038 | 0.46 × 0.094 × 0.034 | 0.492 × 0.168 × 0.034 |
| Radiation | Mo Kα (λ = 0.71073) | Mo Kα (λ = 0.71073) | Mo Kα (λ = 0.71073) |
| 2Θ range for data collection/° | 6.67 to 69.832 | 6.584 to 61.016 | 6.584 to 50.054 |
| Index ranges | -23 ≤ h ≤ 23, -33 ≤ k ≤ 36, -38 ≤ l ≤ 39 | -17 ≤ h ≤ 17, -33 ≤ k ≤ 33, -74 ≤ l ≤ 74 | -14 ≤ h ≤ 14, -27 ≤ k ≤ 27, -61 ≤ l ≤ 61 |
| Reflections collected | 259919 | 275806 | 132298 |
| Independent reflections | 60886 [$R_{int}$ = 0.0593, $R_{sigma}$ = 0.0419] | 45889 [$R_{int}$ = 0.1693, $R_{sigma}$ = 0.1170] | 26382 [$R_{int}$ = 0.1120, $R_{sigma}$ = 0.0689] |
| Data/restraints/parameters | 60886/0/1927 | 45889/0/895 | 26382/4/819 |
| Goodness-of-fit on $F^2$ | 1.038 | 1.078 | 1.101 |
| Final R indexes [I>=2σ (I)] | $R_1$ = 0.0337, $wR_2$ = 0.0941 | $R_1$ = 0.1319, $wR_2$ = 0.3035 | $R_1$ = 0.2251, $wR_2$ = 0.5073 |
| Final R indexes [all data] | $R_1$ = 0.0436, $wR_2$ = 0.0980 | $R_1$ = 0.1744, $wR_2$ = 0.3237 | $R_1$ = 0.2324, $wR_2$ = 0.5105 |
| Largest diff. peak/hole / e Å$^{-3}$ | 2.59/-2.74 | 5.77/-5.27 | 9.78/-7.42 |

**Table S4.** Crystallographic table of the Pr(III) and Nd(III) complexes of $P_2W_{17}$.

| Identification code | PrP2W17-K_mP | NdP2W17-K_aP |
|---|---|---|
| **Empirical formula** | $K_{17}O_{122}P_4PrW_{34}$ | $K_{17}NdO_{126}P_4W_{34}$ |
| **Formula weight** | 9132.39 | 9199.72 |
| **CCDC ID** | 2513144 | 2513145 |
| **Temperature/K** | 298 | 298 |
| **Crystal system** | monoclinic | triclinic |
| **Space group** | $P2_1/n$ | P-1 |
| **a/Å** | 12.3680(2) | 14.6662(2) |
| **b/Å** | 23.4873(4) | 22.5839(3) |
| **c/Å** | 52.0070(11) | 24.8540(3) |
| **α/°** | 90 | 95.3761(12) |
| **β/°** | 90.7538(15) | 102.7173(12) |
| **γ/°** | 90 | 99.6858(12) |
| **Volume/Å$^3$** | 15106.2(5) | 7842.2(2) |
| **Z** | 4 | 2 |
| **$\rho_{calc}$g/cm$^3$** | 4.015 | 3.896 |
| **μ/mm$^{-1}$** | 26.684 | 25.724 |
| **F(000)** | 15736 | 7934 |
| **Crystal size/mm$^3$** | 0.435 × 0.128 × 0.024 | 0.026 × 0.024 × 0.015 |
| **Radiation** | Mo Kα (λ = 0.71073) | Mo Kα (λ = 0.71073) |
| **2Θ range for data collection/°** | 6.578 to 61.016 | 6.684 to 69.656 |
| **Index ranges** | -17 ≤ h ≤ 17, -32 ≤ k ≤ 33, -68 ≤ l ≤ 74 | -23 ≤ h ≤ 23, -34 ≤ k ≤ 35, -39 ≤ l ≤ 36 |
| **Reflections collected** | 216370 | 248578 |
| **Independent reflections** | 45698 [$R_{int}$ = 0.1070, $R_{sigma}$ = 0.0669] | 60224 [$R_{int}$ = 0.1970, $R_{sigma}$ = 0.1110] |
| **Data/restraints/parameters** | 45698/0/1430 | 60224/0/1585 |
| **Goodness-of-fit on F$^2$** | 1.079 | 1.041 |
| **Final R indexes [I>=2σ (I)]** | $R_1$ = 0.1527, $wR_2$ = 0.3729 | $R_1$ = 0.0873, $wR_2$ = 0.2480 |
| **Final R indexes [all data]** | $R_1$ = 0.1672, $wR_2$ = 0.3792 | $R_1$ = 0.1106, $wR_2$ = 0.2699 |
| **Largest diff. peak/hole / e Å$^{-3}$** | 6.88/-4.83 | 7.01/-6.29 |

**Table S5.** Lists of actinide-oxygen bond distances in the Wells-Dawson complexes with Am(III) and Cm(III) reported in the present study. See Sokolova et al.[5] for the Am(IV) structure. The continuous symmetry operation measure (CSoM values) were calculated using the theoretical framework defined by Nielsen & Sørensen.[7] Bond distance and uncertainty values are given in Å.

| **$K_{17}Am^{III}(P_2W_{17}O_{61})_2 \cdot 42.5H_2O$ (Triclinic)** | | |
|---|---|---|
| Am1 | O9 | 2.377 |
| Am1 | O36 | 2.451 |
| Am1 | O37 | 2.399 |
| Am1 | O56 | 2.424 |
| Am1 | O59 | 2.442 |
| Am1 | O62 | 2.441 |
| Am1 | O73 | 2.450 |
| Am1 | O77 | 2.478 |
| **Average** | | **2.433** |
| **Uncertainty** | | **0.005** |
| **CSOM** | | **0.323** |

| **$H_6K_{10}Am^{IV}(P_2W_{17}O_{61})_2 \cdot 30H_2O$ (Triclinic)** | | |
|---|---|---|
| Am1 | O1 | 2.318 |
| Am1 | O2 | 2.380 |
| Am1 | O3 | 2.355 |
| Am1 | O4 | 2.296 |
| Am1 | O62 | 2.271 |
| Am1 | O63 | 2.337 |
| Am1 | O64 | 2.322 |
| Am1 | O65 | 2.322 |
| **Average** | | **2.325** |
| **Uncertainty** | | **NA** |
| **CSOM** | | **0.612** |

| **$K_{17}Am^{III}(P_2W_{17}O_{61})_2 \cdot 12H_2O$ (Monoclinic)** | | |
|---|---|---|
| Am01 | O2 | 2.519 |
| Am01 | O21 | 2.442 |
| Am01 | O28 | 2.406 |
| Am01 | O34 | 2.435 |
| Am01 | O49 | 2.418 |
| Am01 | O76 | 2.493 |
| Am01 | O106 | 2.460 |
| Am01 | O119 | 2.426 |
| **Average** | | **2.450** |
| **Uncertainty** | | **0.027** |
| **CSOM** | | **0.422** |

| **$K_{17}Cm^{III}(P_2W_{17}O_{61})_2 \cdot 8H_2O$ (Monoclinic)** | | |
|---|---|---|
| Cm1 | O19 | 2.437 |
| Cm1 | O26 | 2.360 |
| Cm1 | O32 | 2.481 |
| Cm1 | O47 | 2.412 |
| Cm1 | O110 | 2.455 |
| Cm1 | O113 | 2.345 |
| Cm1 | O116 | 2.557 |
| Cm1 | O98 | 2.508 |
| **Average** | | **2.444** |
| **Uncertainty** | | **0.07** |
| **CSOM** | | **0.901** |

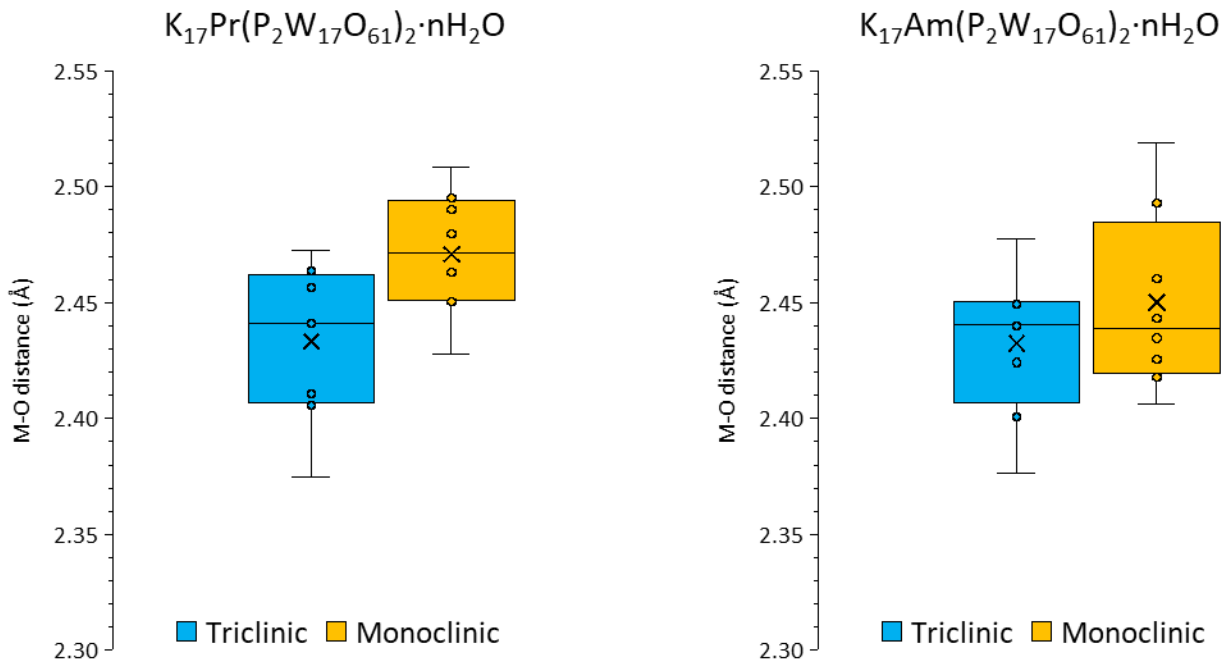


**Figure S3.** Box plots comparing the metal-oxygen bond length distribution for $K_{17}Pr(P_2W_{17}O_{61})_2 \cdot nH_2O$ and $K_{17}Am(P_2W_{17}O_{61})_2 \cdot nH_2O$ in their monoclinic and triclinic phases. The monoclinic phase leads to statistically longer metal-oxygen bonds. We reported the triclinic phase of $K_{17}Pr(P_2W_{17}O_{61})_2 \cdot nH_2O$ elsewhere.[8]

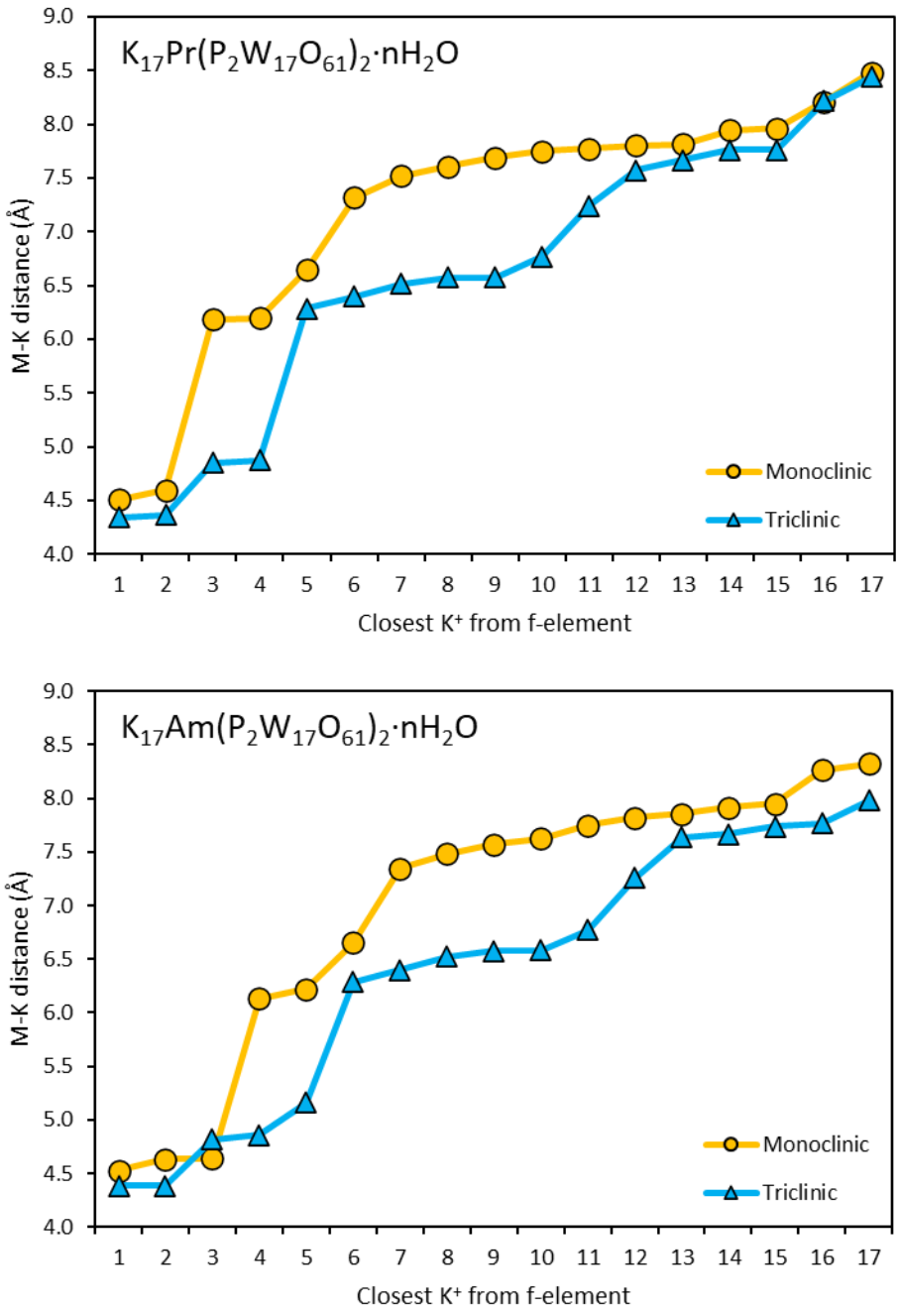


**Figure S4.** Distances between the 17 potassium counterions and the f-element in $K_{17}Pr(P_2W_{17}O_{61})_2{\cdot}nH_2O$ and $K_{17}Am(P_2W_{17}O_{61})_2{\cdot}nH_2O$, for the monoclinic and triclinic phases. In the monoclinic phase, the $K^+$ counterions are further away from the f-element. We reported the triclinic phase of $K_{17}Pr(P_2W_{17}O_{61})_2{\cdot}nH_2O$ elsewhere.[8]

# Materials and methods

***Caution!*** *$^{243}$Am, $^{248/246}$Cm, as well as their decay products, constitute serious health hazards because of their radioactive and chemical properties. Experiments with these radioisotopes were conducted at Lawrence Livermore National Laboratory in facilities designed for the safe handling of short-lived and long-lived radioactive materials and associated waste.*

**Materials.** Curium samples (97% $^{248}$Cm + 3% $^{246}$Cm + 0.01% $^{247}$Cm) were prepared from a primary source purchased from Oak Ridge National Laboratory (USA) and $^{243}$Am(III) chloride purchased from Eckert & Ziegler (USA). Non-radioactive chemicals (e.g., $Na_2WO_4 \cdot 2H_2O$, $NaCH_3COO \cdot 3H_2O$, KCl) were purchased from chemical providers (VWR and Millipore Sigma) and used as received. $K_{10}P_2W_{17}O_{61} \cdot 20H_2O$ was prepared by first isolating the $K_6P_2W_{18}O_{62}$ precursor, as per the method from Contant et al.[9] All solutions were prepared using deionized water purified by reverse osmosis cartridge system (≥ 18.2 MΩ.cm). All experiments were performed in a temperature-controlled room (22°C) and under air atmosphere.

**Synthesis**. The $Am^{III}(P2W17)_2$ and $Cm^{III}(P2W17)_2$ complexes were prepared in situ by directly mixing the stoichiometric amount of the POM and the actinides. Samples were buffered at pH 4.5 with 0.1 M sodium acetate. For crystallization, the syntheses were performed with 100 µL samples containing 13 µM of the complex. This corresponds to 324 nanograms for $^{243}$Am and 330 nanograms for $^{248}$Cm. Despite the low mass of the actinide, single crystals of reasonable size were obtained (See Figure 1). Crystallization was triggered by addition of KCl to the sample, up to a concentration of 3 M. The crystals appear after about 24 hours. The $Am^{III}(P2W17)_2$ appear orange while the $Cm^{III}(P2W17)_2$ crystals appear transparent. The best crystals were harvested from their mother liquor and mounted on crystallography pins for scXRD analysis. Presence of radioisotope in the mounted crystals was done on the spot with radiological probes. Similar crystals were analyzed via Raman microscopy and solid-state UV-vis absorbance. TGA analysis could not be performed on the crystals due to the small scale of the synthesis and radioactive nature of the samples.

**Solution-state UV-visible-NIR spectrophotometry.** Absorbance spectra of the aqueous samples were measured using a high-performance Cary 6000i UV-vis-NIR spectrophotometer (Agilent

Technologies). Samples were contained in cuvettes with a path length of 10 mm. Spectra were corrected blank by measuring the absorbance of the corresponding buffer prior to each titration.

**Solid-state UV-visible spectrophotometry.** Absorbance spectra of the solid samples were measured using a CRAIC Technology 508 PV$^{TM}$ microspectrophotometer. Crystals were isolated from their mother liquor and the analysis was performed on multiple crystals to check for consistency. Crystals of the same compound and same crystal morphology gave similar spectra. The spectral window was 400–900 nm as accessible by the white the light source of the instrument. The reported spectra are averages of at least 100 scans, with an integration time per scan optimized by the instrument software for each sampling area.

**Raman Microscopy.** Raman spectra were collected using a Senterra II confocal Raman microscope (Bruker), equipped with high resolution gratings (1,200 lines/mm) and a 532 nm laser source (operated at 15 mW), and a TE-cooled CCD detector. Reported spectra are the average of at least 5-10 different spots per sample, each spot analysis consisting of 64 scans. Multiple crystals of the studied compound were analyzed to confirm the reproducibility of the results. The integration time was set to 100 ms per scan. The sampling area was visually inspected using the microscope camera before and after the Raman data collection. No damage to the sample was observed due to the laser irradiation.

**Crystallography.** The structure was collected using a Rigaku Synergy-S single crystal diffractometer, equipped with a kappa goniometer and using Mo Kα radiation (λ = 0.71073 Å) with a FWHM of ~200 μm at the sample from a microfocus source. Images were recorded on a Dectris Pilatus 3R (300K – CdTe) detector and processed using CrysAlis$^{Pro}$. After integration both analytical absorption and empirical absorption (spherical harmonic, image scaling, detector scaling) corrections were applied.[10] The structure was solved by Intrinsic Phasing method from SHELXT program[11], developed by successive difference Fourier syntheses, and refined by full-matrix least square on all $F^2$ data using SHELX[12] via OLEX2 interface[13]. Crystallographic information for the reported structure can be obtained free of charge from the Cambridge Crystallographic Data Center (https://www.ccdc.cam.ac.uk/) upon referencing the CCDC numbers 2512143, 2512144, 2512145, 2512146, or 2512147. Further details on the crystallographic results are given in the ESI.

**Notes on crystal structures, refinement, modeling of disorder, and solvent void space.**
Due to safety protocols, any transuranic-containing crystals were collected under the MicroRT Capillaries 37mm. Although x-ray transparent at certain angles the background intensity increased resulting in poor signal-to-noise ratio, resulting in the use of some restraints.

Absorption correction was performed using Empirical absorption correction applied before frame scaling. Several other methods were employed, such as numerical absorption with a Gaussian grid (based on the crystal system), or analytical absorption correction after the Clark and Reid method before ultimately using a combination of Gaussian grid absorption correction and "Mutli-scan" using the Scale3 Abspack. All of these methods rely on measuring the face of the crystal using CCD images captured before data collection. The resulting $R_{int}$ after absorption correction dropped for each structure by approximately 3%. Nevertheless, large residual electron density less than 1 Å away from the tungsten atoms remained. However, this resulted in some No Positive Displacement parameters for some oxygens atoms. For troublesome structures, the EADP constraint was used on oblate, prolate and NPD oxygen atoms. When the constraint was used a R1 increase of about 0.5 % was seen. A such it was deemed reasonable to use the constraints for two of the structures reported here (CCDC ID 2513147 and 2513143).

Furthermore, individual hydrogen atoms could not be refined, as such they have been omitted in the reported molecular weight.

**Common cif alerts and responses thereof**

- **PLAT971/2/3_ALERT_2_A Check Calcd Resid. Dens. X Ang from X**
  Response: High residual Q-peaks of 0.1*Z/Å$^3$ at 0.6 – 1.2 Å away from the heavy atoms (15). While most structures are within this range, we nevertheless processed the data through several different absorption correction methods before ultimately using spherical or multi-scan methods. (15)
- **PLAT910_ALERT_3_B Missing # of FCF Reflection(s) Below Theta(Min).**
  Response: Missing hkl reflection missing due to beam stop mask applied to detector during data collection while at minimal distance allowed by the instrument. As such, a decision was taken to sacrifice a few reflections for higher overall intensity, due to the size and synthesis nature of the crystals.

- **PLAT306_ALERT_2_B Isolated Oxygen Atom (H-atoms Missing ?)**
  Response: solvent water molecules, H-atoms not located.

Individual cases are discussed below.

# References


1 C. Zhang, L. Bensaid, D. McGregor, X. Fang, R. C. Howell, B. Burton-Pye, Q. Luo, L. Todaro and L. C. Francesconi, *J Clust Sci*, 2006, **17**, 389–425.

2 K. Hirakawa, Y. Sekine, F. Kobayashi, Y. Horii, H. Zenno, M. Nakaya and S. Hayami, *Crystal Growth & Design*, 2025, **25**, 2163–2171.

3 J. Niu, J. Zhao, D. Guo and J. Wang, *Journal of Molecular Structure*, 2004, **692**, 223–229.

4 Q.-H. Luo, R. C. Howell, M. Dankova, J. Bartis, C. W. Williams, Horrocks William DeW., Young Victor G., A. L. Rheingold, L. C. Francesconi and M. R. Antonio, *Inorg. Chem.*, 2001, **40**, 1894–1901.

5 M. N. Sokolova, A. M. Fedosseev, G. B. Andreev, N. A. Budantseva, A. B. Yusov and P. Moisy, *Inorg. Chem.*, 2009, **48**, 9185–9190.

6 A. Ostuni, R. E. Bachman and M. T. Pope, *Journal of Cluster Science*, 2003, **14**, 431–446.

7 V. R. M. Nielsen and T. Just Sørensen, *Nat Commun*, 2025, **16**, 11122.

8 I. Colliard and G. Deblonde, *ChemRxiv*, 2025, preprint, DOI: 10.26434/chemrxiv-2025-ct10m.

9 R. Contant, W. G. Klemperer and O. Yaghi, in *Inorganic Syntheses*, John Wiley & Sons, Ltd, 1990, pp. 104–111.

10 G. M. Sheldrick, Bruker-Siemens area Detection Absorption other Correction (version 2008/12008) 2008.

11 G. M. Sheldrick, *Acta Cryst A*, 2015, **71**, 3–8.

12 G. M. Sheldrick, *Acta Cryst A*, 2008, **64**, 112–122.

13 O. V. Dolomanov, L. J. Bourhis, R. J. Gildea, J. a. K. Howard and H. Puschmann, *J Appl Cryst*, 2009, **42**, 339–341.